Journal of Vegetation Science 9: 445-454, 1998

Computerized classification of Mediterranean vegetation using panchromatic aerial photographs

Carmel, Yohay & Kadmon, Ronen

Department of Evolution, Systematics and Ecology, The Hebrew University of Jerusalem, Jerusalem 91904, Israel; Fax +972 2 6584741; E-mail yochaym@suma.bot.huji.ac.il

Abstract. Historical aerial photographs are an important source for data on medium- to long-term (10 - 50 yr) vegetation changes. Older photographs are panchromatic, and manual interpretation has traditionally been used to derive vegetation data from such photographs. We present a method for computerized analysis of panchromatic aerial photographs, which enables one to create high resolution, accurate vegetation maps. Our approach is exemplified using two aerial photographs (from 1964 and 1992) of a test area on Mt. Meron, Israel. Spatial resolution (pixel size) of the geo-rectified photos was 0.30 m and spatial accuracy (RMS error) ca. 1 m. An illumination adjustment prior to classification was found to be essential in reducing misclassification error rates. Two classification approaches were employed: a standard maximum-likelihood supervised classifier, and a modification of a supervised classification, which takes into account spectral properties of individual pixels as well as their neighbourhood characteristics. Accuracy of the maximum likelihood classification was 81 % in the 1992 image and 54 % in the 1964 image. The neighbour classifier increased accuracy to 89 % and 82 % respectively. The overall results suggest that computerized analysis of sequences of panchromatic aerial photographs may serve as a valuable tool for the quantification of medium-term vegetation changes.

Keywords: GIS; Image analysis; Neighbour classifier; Remote sensing; Vegetation dynamics.

Abbreviations: DEM = Digital Elevation Model; RMS = Root Mean Square.

Introduction

The study of medium-to long-term vegetation changes (10 - 50 yr) is important for understanding ecological processes, notably succession (e.g. Debussche et al. 1996; Callaway & Davis 1993; see also Bakker et al. 1996), forest degradation (e.g. Ross et al. 1994), animal distribution changes (e.g. Berger & Baydack 1992), as well as for the planning of vegetation and wildlife management programs (e.g. Keane et al. 1997). One source of data for such studies is aerial photographs; these may have a high spatial resolution and may cover a long time sequence. Large-scale photos (1:10 000 to 1:15 000) are available for many areas, and objects of 10 to 20 cm in size can be identified in them (Fig. 1). High quality panchromatic (black/white) photos can be found for the last 50 to 60 years for many parts of the world. Thus, aerial photos are commonly used for studies of medium-term vegetation changes (e.g. Scanlan & Archer 1991; Callaway & Davis 1993; Frelich & Reich 1995; Hester et al. 1996) . Past investigations have typically employed manual interpretation of aerial photographs to extract vegetation data. The labour-intensive nature of manual interpretation may limit the spatial extent of vegetation databases (Woien 1995). Manually interpreted maps usually have coarse spatial resolution, and classification accuracy, which is a critical parameter for studies of vegetation change, is not readily assessed in this method (Biging et al. 1991). Manual interpretation of aerial photos is assumed to be 100 % correct, which is not true (Biging et al. 1991; Congalton & Green 1993).

Computerized vegetation classification of panchromatic aerial photographs has rarely been done (Stephens 1985; Short & Short 1987). In applying computerized methods to analyse vegetation data from aerial photographs one faces several difficulties. The classification of a panchromatic aerial photograph is a special case of remote sensing image classification involving only one band, the grey level. Naturally, the accuracy of common classification methods decreases seriously when only one band is used (Short & Short 1987). Another problem is that the illumination changes across the scene (Short & Short 1987; Dymond 1988, 1992).

In this paper we present a computerized method for generating time series of high resolution, accurate maps of Mediterranean vegetation using panchromatic aerial photographs. Our classification scheme follows Tomaselli (1977) and includes three classes, based on vegetation height: woody vegetation > 2.5 m (‘trees’), woody vegetation < 2.5 m, including shrubs, semi-shrubs and low trees (‘shrubs’), and herbaceous vegetation, including bare ground. The applicability of our approach is evaluated using two photographs (1964 and 1992) of a test area on Mt. Meron, Israel. The pre-classification process included photomap preparation and illumination adjustments. Two classification approaches were applied: (1) Maximum-likelihood supervised classification and (2) A

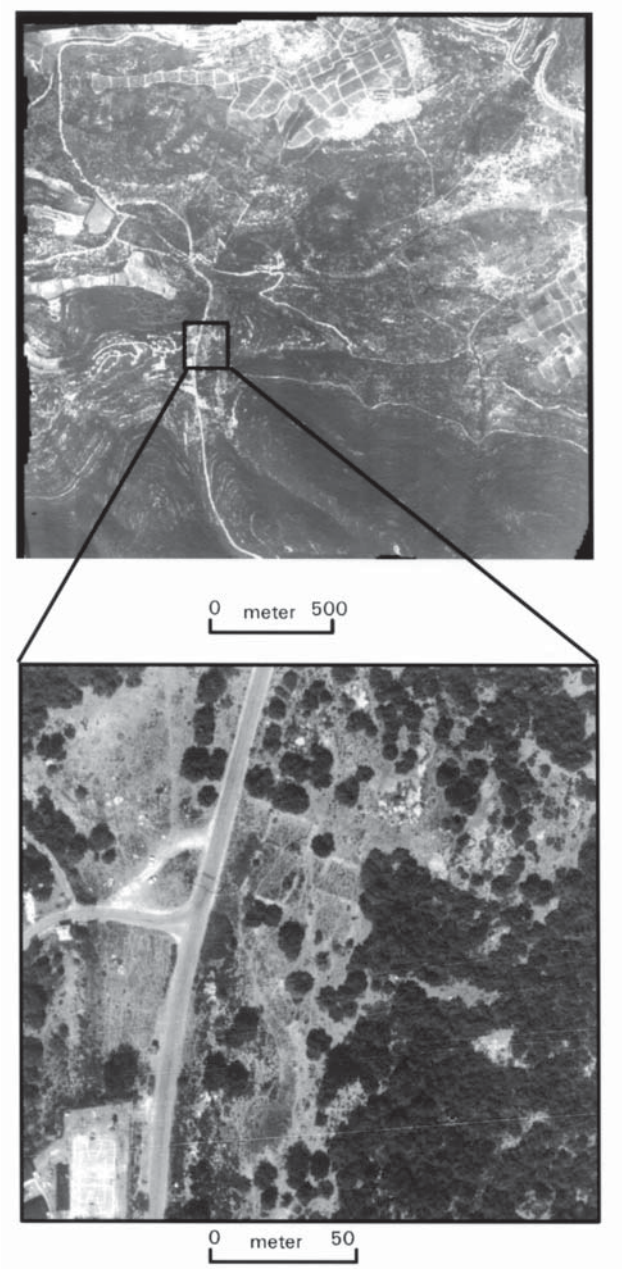

Fig. 1. Study area. **a.** The entire study area in the 1992 aerial photograph. **b.** Small part of the photo enlarged. Elements like small shrubs and lines on a basketball field (bottom left) can be distinguished.

classification algorithm which takes into account grey levels of individual pixels as well as their neighbourhood characteristics (termed here 'neighbour classification'). We hypothesize that accounting for the spatial aspects of grey level distribution should increase classification accuracy. Results of the two classifications are compared with an extensive ground-truthing database.

Methods

Study area

An area of 400 ha on the northern slopes of Mt. Meron, Upper Galilee Mountains, Israel (32° N, 35° E) was chosen. The study area is heterogeneous in terms of topography (altitude range 650 - 950 m) and vegetation structure. The dominant tree, shrub and semi-shrub species are *Quercus calliprinos*, *Calicotome villosa* and *Sarcopoterium spinosum*, respectively. The entire area has been subject to intensive grazing and tree harvesting regimes, which have been largely reduced since 1948. Two aerial photographs (1964 and 1992) were chosen, and obtained from the Israel Mapping Center. Both photos were taken in summer around noon. The scale of the earlier photo is 1:14 000 and that of the later one is 1:12 000. Diapositives of the photos were scanned using an RM-1 high resolution scanner (Wherli Associations). Scaning resolution was 12 μ, and thus each pixel represented 15 cm × 15 cm on the ground. Anthropogenic elements – roads, settlements and agricultural areas, which together comprised < 15 % of the study area – were manually digitized on the photos, and excluded from further analysis.

Photomap preparation

In the ortho-rectification process, the radial, tilt and relief distortion inherent in aerial photos are removed, and the photograph is registered to a planimetric coordinate system (Dymond 1986; Bolstad 1992). Ground control points were identified on both photos and in the field. Points were measured using a Magellan ProMARK X CP ™ GPS receiver (Anon. 1994), using the differential mode. Distance between base station and the mobile receiver did not exceed 4 km. Data were analyzed for differential corrections using carrier phase mode in the Magellan MSTAR software (Anon. 1994). Accuracy of the ground control points was estimated using four independent triangulation points in the study area, for which accurate coordinates were obtained from the Israel Mapping Center.

DEM of the study area was prepared using a pair of partially overlapping photos from 1992, and another DEM of the same area was prepared using a corresponding pair of photos from 1964. Both DEMs were constructed with ISMT® software of INTEGRAPH Inc. (Huntsville, USA) at a spatial resolution of 10 m. Root Mean Square (RMS) error was calculated separately for each stereoscopic model. Each photomap was then prepared using its own DEM, in order to reduce spatial error. The Photomaps were prepared using ISIR software (INTEGRAPH Inc.). The combined spatial error between the photomaps was measured by superimposing the photomaps and measuring the distance between identical points in the two photomaps. We measured 40 such points that were identifiable on both photomaps. This measure represents the overall spatial error that combines all error sources on both photomaps. RMS errors for the different stages in the preparation of the photomaps are summed in Table 1. The photomaps were imported to ERDAS IMAGINE® v 8.2 (Anon. 1995) for the classification processes. Pixel size of 15 cm resulted in a 500 Mb image, which turned out to be too large for demanding analysis tasks. We therefore used a degradation process (ERDAS degrade function) to set the final pixel size on both photomaps to 30 cm.

Training data acquisition

Using 10-fold enlargements of the 1992 photo, we identified patches of trees, shrubs and herbaceous vegetation in the field and drew their boundaries on the photo-enlargements. At this scale, even small shrubs could be identified in the field. In this way we collected signatures of the three vegetation classes defined above. Signatures were collected from a variety of regions throughout the study area. For the 1964 image we could not, of course, identify vegetation elements in the field. Training sets for the 1964 photo were therefore prepared using an IMD digital stereo plotter (Image-Station 6400, INTEGRAPH Inc.), which enables on-screen measurement of heights of individual shrubs and trees. Vegetation elements identified in this way were used to define signatures for their respective vegetation category.

Illumination adjustments

The major source of uneven illumination in remotely sensed images is the topographic effect (Teillet et al. 1982). We used the 'topographic normalization' process (Anon. 1995), which is based on a Minnaert model (Teillet et al. 1982), to correct slope and aspect effects on radiance. Preliminary results indicated that this process improved classification accuracy in specific regions on the photos, but decreased accuracy in other regions. Its overall effect was a slight reduction in classification

Table 1. Planimetric errors of the different stages in photomap preparation, in m. The GPS measurement error is an estimation, see text.

Source of error	RMS	Largest error
GPS measurements	0.23	0.32
1964 stereoscopic model	0.75	-
1992 stereoscopic model	0.75	-
Overall between-photomap error	1.13	1.64

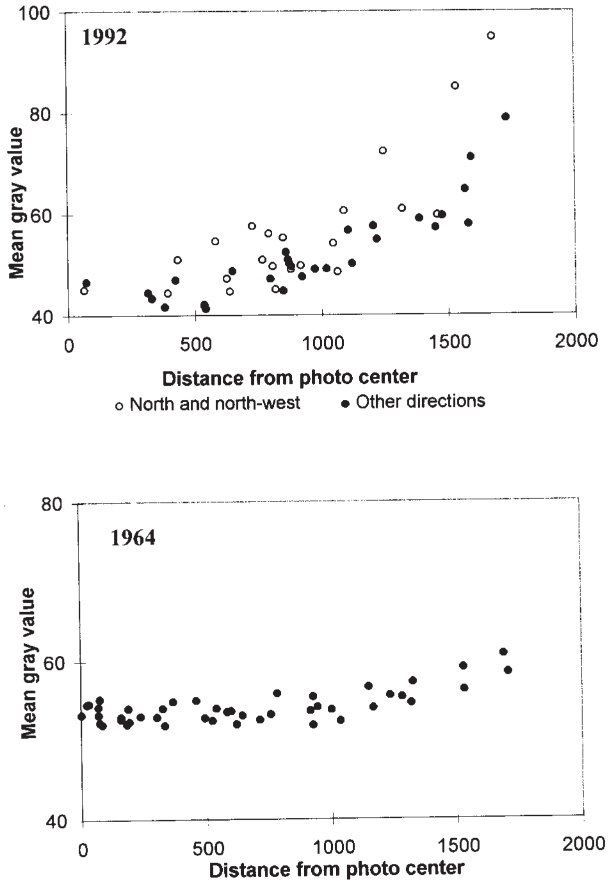

Fig. 2. Mean grey level of trees, as a function of their distance from the image center.

accuracy, therefore it was not applied to the images.

While running preliminary classification trials, we noticed another source of illumination distortions in the images. We found a gradual increase in grey levels of similar objects (trees, shrubs and bare rocks) from the center towards the periphery of the photo, presumably due to directional reflectance effects (Dymond & Trotter 1997). This effect could hardly be detected by a visual inspection of the photo, but had a crucial effect on the classification results. The phenomena appeared on both photos, but was more pronounced on the 1992 photo. Two standard methods (Fourier transformation and brightness adjustments; Anon. 1995) were used to correct this attenuation, but none of them corrected the image successfully. We therefore developed a simple correction algorithm, based on distance from photo center. We identified in the field 51 oak trees that were scattered over the whole 1992 image, and digitized their boundaries on the image. For each tree we calculated the distance and azimuth from the image center, and the mean of its grey level values (using IMAGINE signature editor;

Anon. 1995). A plot of mean grey level against distance from center indicated that a linear relationship existed between these parameters, for distances larger than 600 m, while for smaller distances no such relationship existed (Fig. 2). Also, in the 1992 image there was a clear difference between mean grey level of trees in directions N and NW (315 - 360) and all other directions (Fig. 2a). Using linear regression we determined the effect of distance from center on mean grey level values of trees, for distances > 600 m. Regression equations were calculated separately for trees in directions N and NW and for all other directions together (Table 2a). We used the regression parameters to calculate an adjustment factor for each pixel based on its distance and direction from the image center. The Arc-Info AML language (Anon. 1996) was used to write a program for this correction, which uses the Arc-Info GRID module as a platform. The 1964 image was corrected in a similar manner, with two exceptions: tree identification was made using a digital stereo plotter as explained above, and no directional biases were found (Fig. 2b), resulting in a single equation (Table 2b). Fig. 3 shows the distributions of pixel values in signatures derived from training sets of the three classes (trees, shrubs and herbaceous vegetation) on the 1992 image before and after the illumination adjustments.

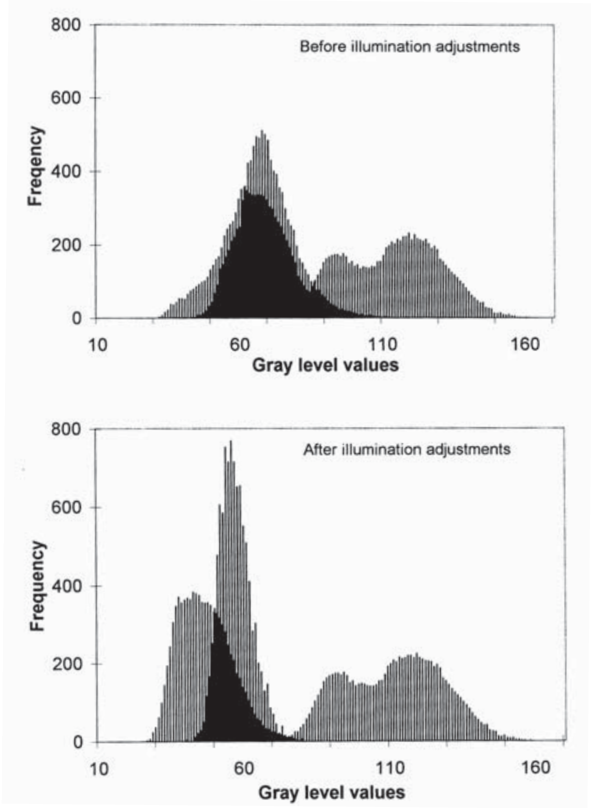

Fig. 3. Grey level distribution of signatures of trees, shrubs and herbaceous vegetation on the 1992 photograph, before and after illumination adjustments.

Classification methods

Two image classification methods were compared in this study. A maximum-likelihood supervised classifier (Anon. 1995) was employed using signatures of trees, shrubs and herbaceous vegetation, derived from the training sets. The second method is an algorithm which accounts also for the neighbourhood characteristics of individual pixels (termed here 'neighbour classifier').

Histograms of the three vegetation classes indicate that in general, trees appear darker than shrubs, which in turn are darker than herbs (Fig. 3). However, there is a considerable overlap between grey level values of neighbouring classes (e.g. trees and shrubs) indicating that any threshold (e.g. the maximum-likelihood classifier) would result in large classification errors in the overlap range. The neighbour approach attempts to reduce these errors, taking into account information about the spatial arrangement of pixels with grey levels in the overlap range. First, the image was classified into three classes (Fig. 4): Class 1 consists of pixels which belong to 'tree', class 2 consists of pixels belonging to either 'tree' or 'non-tree' and class 3 consists of 'non-tree' pixels. Comparing this classified image with our field based vegetation map, we noticed that most of the tree clumps in the image (more than 99 %) had some class-1 pixels within their canopy boundaries (Fig. 5c). Based on this feature, we used a 'focal minimum' circle window, to tag as trees all class 2 pixels that were in a 'proper proximity' to class 1 pixels. 'Proper proximity' was defined as the canopy radius of a single small tree (1.5 m = 5 pixels).

Once trees had been tagged, the same process was applied to distinguish between shrubs and herbs. This time, the image (except 'trees') was classified into three

Table 2. Results of regressing mean-tree-signature on distance-from-photo-center, for distances larger than 600 m. See also Fig. 2.

Direction	Adjusted R square	Regression coefficient	P-value
a. 1992 photomap			
All directions	0.61	0.027	< 0.0001
North and North-West	0.84	0.039	< 0.0001
All other directions	0.78	0.022	< 0.0001
b. 1964 photomap			
All directions	0.66	0.006	< 0.001

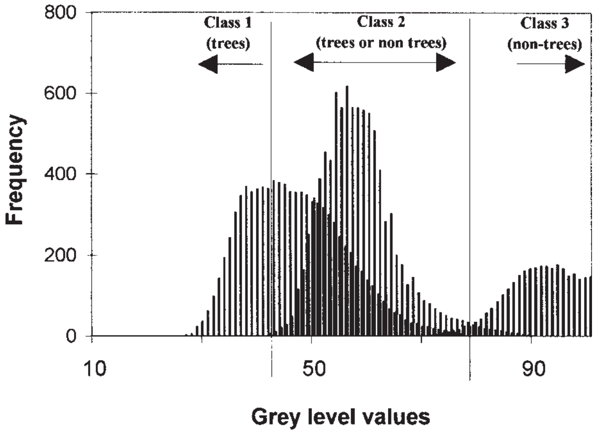

Fig. 4. Thresholds for the first step in the neighbour classifier. Class 1 corresponds to pixels belonging to trees, class 2 includes pixels that could be either trees or non-trees, and class 3 includes non-tree pixels. Gray level values larger than 100, which were all herbaceous, are eliminated from the plot.

classes, 1: shrubs, 2: shrubs or herbs and 3: herbs, followed by a focal minimum window again, which tagged as 'shrubs' all class 2 pixels that were in a 'proper proximity' to class 1 pixels. The 'proper proximity' was re-defined as the radius of a single small shrub (0.3 m = 1 pixel). Pixels which were not classified as either trees or shrubs were then classified as herbaceous vegetation. The main stages of the process are exemplified in Fig. 5.

Ground-truthing database

Detailed ground-truthing vegetation maps for 5 plots, 200 m × 200 m each, were prepared in 1994. We used ten fold enlargements of these plots on the 1992 image to identify all vegetation elements in the field, and delineate their boundaries on the enlargements. The database for 1964 photo was prepared using the IMD digital stereo plotter, as explained above for the training data acquisition. Each woody object in five selected plots in the 1964 image was measured, and its boundary delineated on the photo enlargement. As with the 1992 image, ground truthing vegetation maps were prepared for five 200 m × 200 m plots.

Table 3. Overall accuracy for individual plots.

plot	No. of points	Supervised classification overall accuracy	Neighbor classification overall accuracy
a. 1964 image			
1	101	0.58	0.88
2	95	0.57	0.85
3	111	0.47	0.77
4	104	0.56	0.81
5	105	0.53	0.81
all	516	0.54	0.82
b. 1992 image			
1	83	0.71	0.89
2	103	0.83	0.87
3	128	0.85	0.88
4	137	0.84	0.90
5	120	0.80	0.89
all	571	0.81	0.89

Assessing classification accuracy

Accuracy of each classification method was assessed using random sampling of at least 80 points in each of the five ground truthing plots. A homogeneous 3 × 3 pixel cluster (0.9 m × 0.9 m) was defined as the sampling unit for the accuracy assessment. Overall accuracy was calculated for each plot separately. Differences in accuracy between plots would indicate spatial variability in classification accuracy. These differences were tested using a χ^2 test on a 2 × 5 table of correctly vs. incorrectly classified points in each plot (Sokal & Rohlf 1981). Data from all plots were then pooled to construct a single error matrix for each year. Taken together, 571 and 516 points were used in the 1992 and 1964 images, respectively. The error matrix, overall accuracy, and the κ-statistic (Congalton 1991) were determined for each classification. The Fisher exact test (Sokal & Rohlf 1981) was applied to a 2 × 2 table of correctly vs. incorrectly classified points in each method, to test whether differences between the two methods were statistically significant.

Results

In the 1992 image average overall accuracy was 81 % (cv = 0.07) and 89% (cv = 0.01) for the supervised and neighbour classifiers respectively (Table 3). In the 1964 image average accuracy was 54% (cv = 0.08) and 82% (cv = 0.05) for the supervised and neighbour classifiers respectively. Differences in overall accuracy between plots were not significant (χ^2 test, $p > 0.05$) for all images and classifiers.

The neighbour classification was significantly superior to the maximum-likelihood supervised classification (Fisher exact test, $p < 0.001$ in both images). Classification accuracy for the 1992 image was significantly higher than that of 1964 (Fisher exact test, $p < 0.001$ for both methods). The error matrices for the 1992 image (Table 4a) reveal that the largest error sources in the supervised classification were trees classified as shrubs and shrubs classified as herbaceous vegetation. The neighbour method effectively reduced both error types.

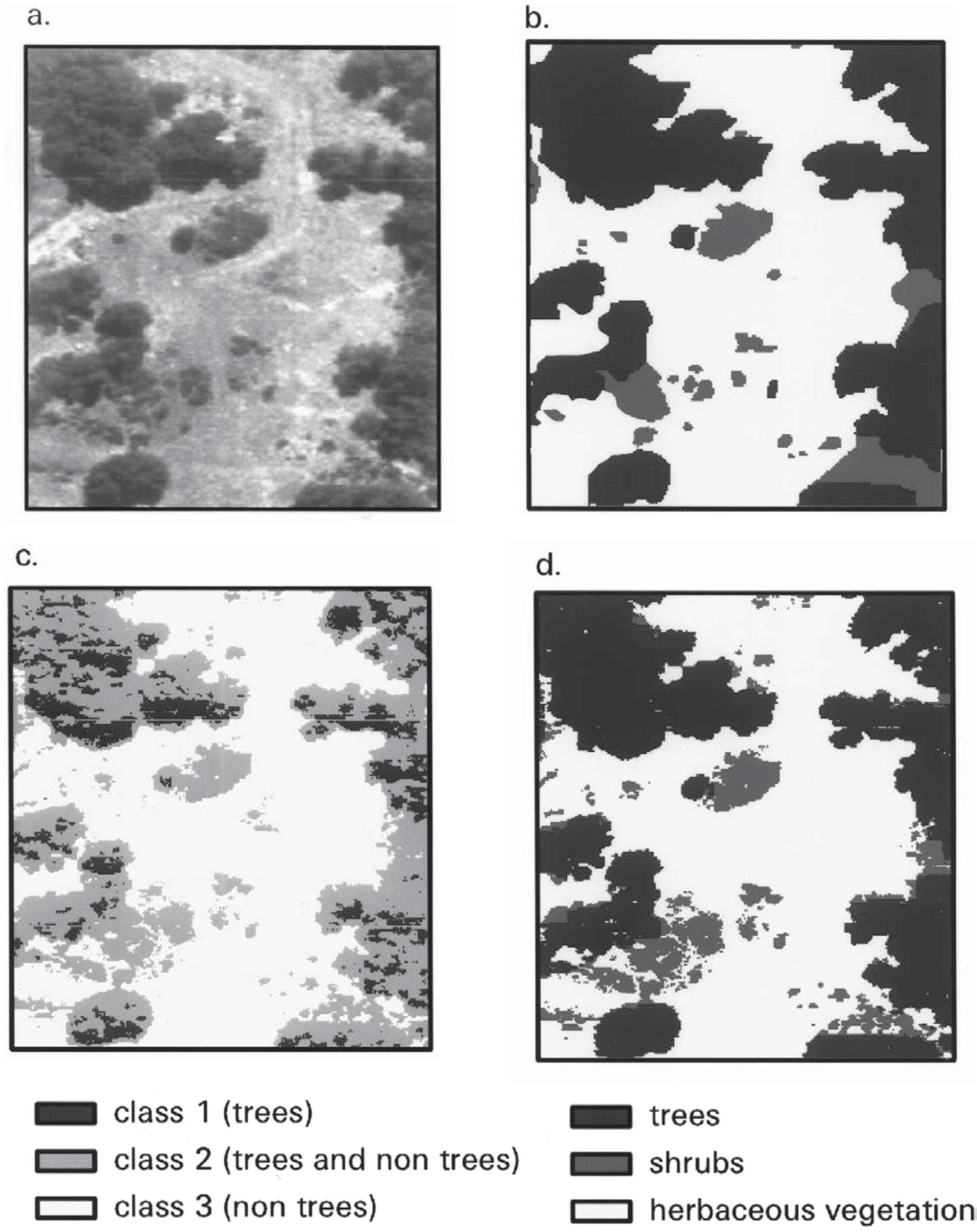

Fig. 5. Main stages in the neighbour classification algorithm, exemplified on a small part of the 1992 image. **a.** The raw image. **b.** Vegetation map, based on a detailed field survey. **c.** The image classified using the thresholds portrayed in Fig. 4. **d.** Final results of the neighbour classification.

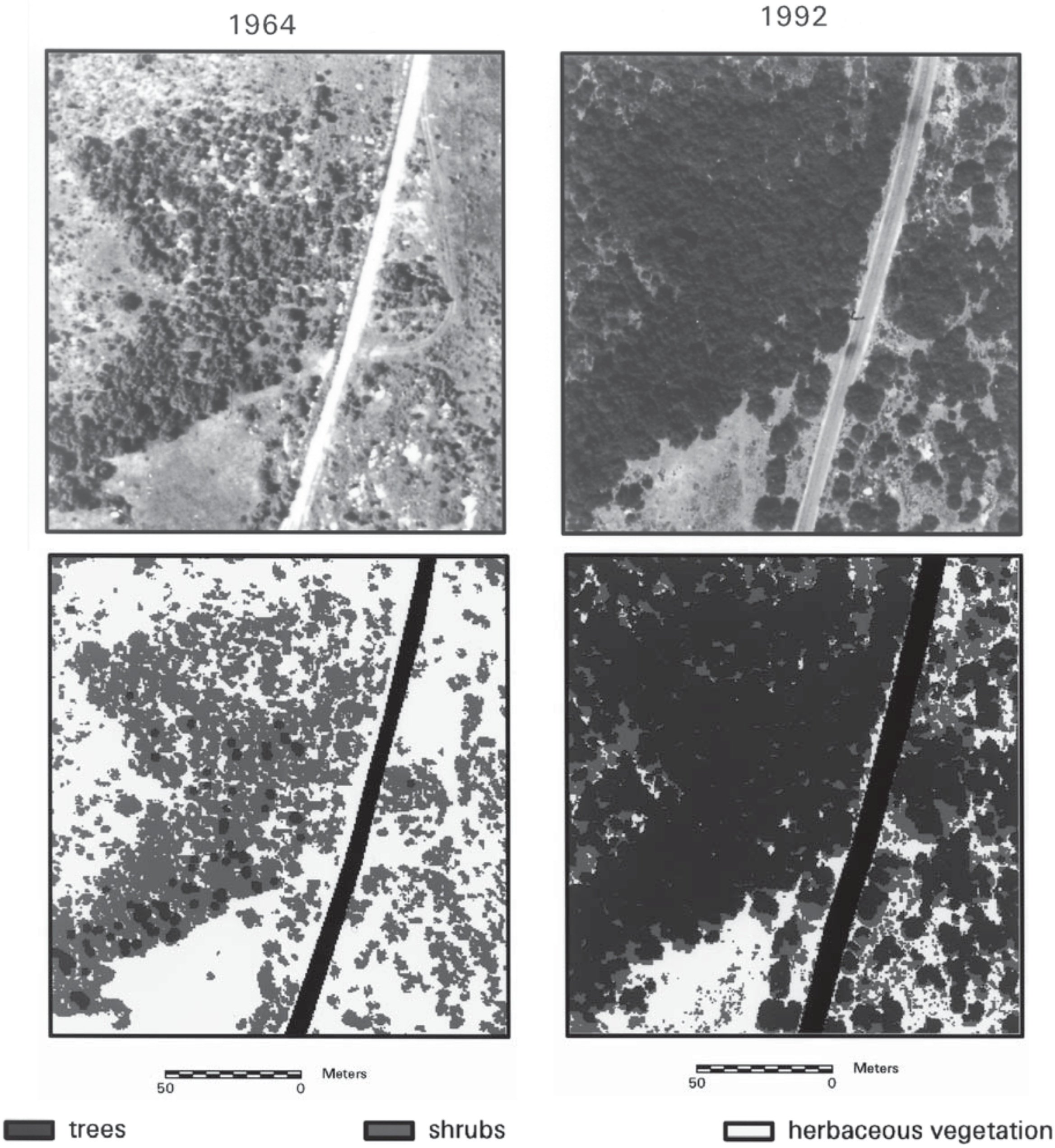

Fig. 6. Small part of the study area; photomaps of the 1964 and 1992 images (top) and their corresponding vegetation maps (bottom), created using the neighbour classifier. The RMS overall spatial error between the two photos is 1.13 m. Pixel size is 30 cm.

The 1964 image was characterized by larger overlaps between spectral signatures of vegetation classes compared with the 1992 image. The largest error sources in the supervised classification of the 1964 image were shrubs classified as herbs and vice versa, while the neighbour classifier has drastically reduced these shrubs/herbs mis-classifications (Table 4b). The κ-coefficient reveals that both methods improved the classification, compared to a random classification (Table 5).

Fig. 6 shows a small part of the 1964 and 1992 photomaps and their corresponding vegetation maps produced using the neighbour classifier. At this high resolution even small trees and shrubs can be identified and changes in individual trees and shrubs can be traced. The vegetation maps produced for the entire study area in 1964 and 1992 are shown in Fig. 7. A considerable change in the vegetation during this 28-yr period emerges from these maps. Trees increased from 2 % cover in 1964 to 41 % in 1992. Herbaceous vegetation cover has

Table 4. Accuracy assessments for supervised and neighbor classifications.

		Supervised classification Reference				Neighbor classification Reference		
		Trees	Shrubs	Herbs		Trees	Shrubs	Herbs
a. 1964 image.								
	Trees	73	40	5	Trees	85	32	3
Classified	Shrubs	36	110	71	Shrubs	25	183	13
	Herbs	8	82	108	Herbs	7	17	168
b. 1992 image.								
	Trees	129	17	0	Trees	156	19	0
Classified	Shrubs	52	90	4	Shrubs	24	109	8
	Herbs	1	33	245	Herbs	1	13	241

diminished from 56 % in 1964 to 24 % in 1992. The vegetation changes that took place in the study area during that period were not uniform; some areas have rapidly changed while other areas remained almost unchanged (Fig. 7).

Discussion

The largest error type in the supervised classification of the 1992 image was tree-shrub misclassification (Table 4b) which corresponds to the considerable overlap between these classes (Fig. 3). These errors were largely reduced when the neighbour classifier was used. Supervised classification of the 1964 image resulted in a relatively low accuracy (54%), probably due to larger overlaps between class signatures. However, the neighbour classifier still produced fair accuracy (82%) for this image. We conclude that the neighbour classifier is less sensitive to overlap between classes than a maximum-likelihood classifier, and thus may be especially useful in cases of single-band images, where large spectral overlap between classes exists.

One important advantage of a computerized approach for vegetation mapping is that accuracy of the classification is being assessed and reported (Congalton 1991). Classification accuracy of vegetation maps based on manual interpretation of aerial photos has seldom been assessed, and error matrices are not reported in any of these studies. Computerized classification of panchromatic aerial photographs has rarely been performed, and we have found only two reports of such works. Stephens (1985) used a supervised method to classify aerial photographs into bare sand, pasture and trees. He reports an overall accuracy of 94% - 95%, and also notes that there was no spectral overlap between these classes, which might explain this high accuracy. Spatial resolution was 1.25 m; spatial accuracy was not assessed. Short & Short (1987) used image analysis to identify oak trees on a panchromatic photo. The classification method was not specified, but it seems to be simple thresholding. Spatial resolution was 3 m, spatial accuracy and classification accuracy were not assessed. To account for illumination variation, they analyzed small patches of the photo separately.

In our study, illumination adjustments, which compensate for the grey values gradient appeared in the photos, were found to be an essential stage before computerized classifications may be applied to an aerial photograph. The Minnaert model we used to correct slope and aspect effects on radiance did not improve the classification results, and we assume that a method which might better account for topographic effects (Dymond 1992) would further improve the classification results.

Medium-term vegetation changes have previously been studied with respect to a variety of ecological issues, including vegetation succession (e.g. Callaway & Davis 1993; Johnson 1994; Aaviksoo 1995), forest degradation (e.g. Strong & Bancroft 1994; Akashi & Mueller-Dombois 1995) and long term animal-plant interactions (Johnston & Naiman 1990; Berger & Baydack 1992). All of these studies constructed their databases using manual interpretation of aerial photos. An ideal database for such studies would cover large areas, and have both high resolution and high spatial accuracy. However, manual interpretation implies a trade-off between these three requirements. Preparation

Table 5. κ-coefficients.

	Supervised classification	Neighbour classification
1964	0.30	0.72
1992	0.71	0.82

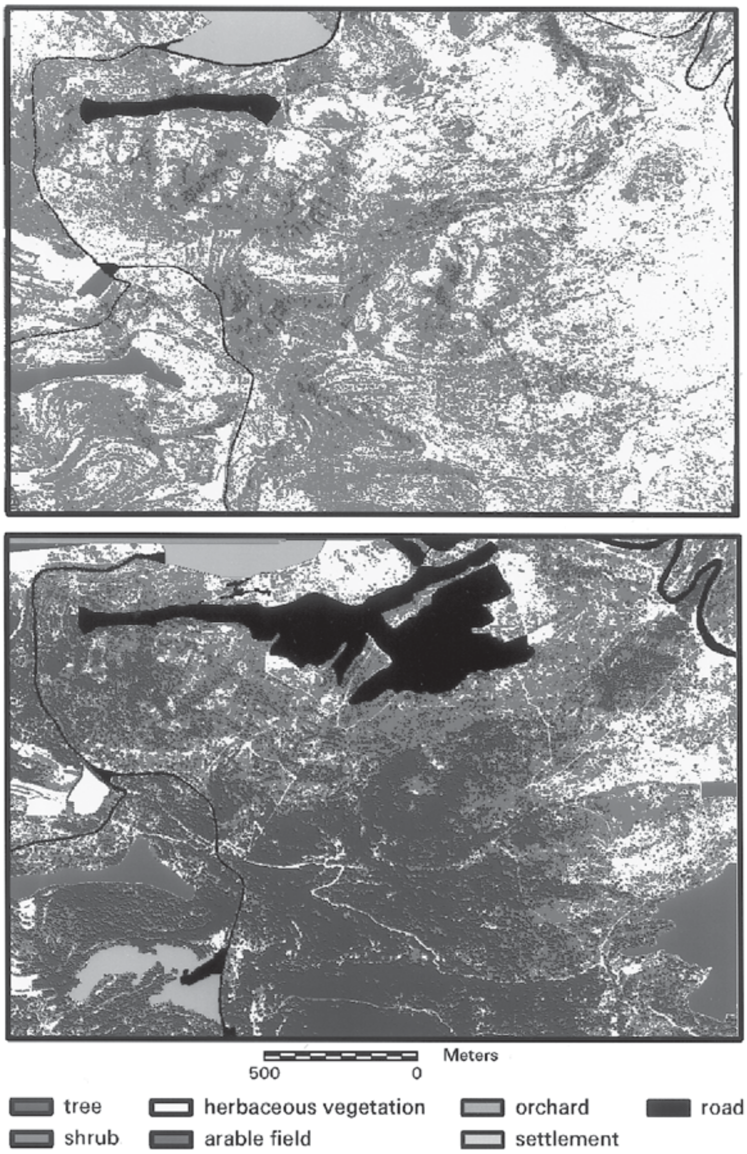

Fig. 7. Vegetation maps of the entire study area in 1964 and 1992. Pixel size is 30 cm.

of a database covering large areas necessarily limits both resolution and accuracy, and vice versa. This study demonstrates that the use of computerized vegetation classification of aerial photographs eliminates this trade-off, and enables one to produce vegetation maps that have high spatial resolution, high spatial accuracy and cover relatively large spatial extent.

In most studies of vegetation change which employed aerial photographs, vegetation maps were prepared by delineating polygons on the photos, and assigning vegetation category to each polygon as a whole. The polygons were then transferred onto maps, usually with the aid of a zoom transfer scope (e.g. Harrington & Sanderson 1994; Frelich & Reich 1995). This procedure culminates in a relatively coarse spatial resolution. In contrast, our approach is based on assigning the type of vegetation element (tree or shrub) to each pixel. An advantage of this method is that it enables one to create maps in which cover estimations can be objectively determined for any polygon of interest (e.g. % of tree cover for specific woodland plots) or for grid cells at any resolution, using simple GIS tools. Moreover, confidence limits can be calculated for these estimations, using parameters derived from the respective error matrices. Such maps of cover estimations for specific plots may be useful for a variety of forestry and ecological applications.

Acknowledgements. This study was funded by Keren Kayemet Leisrael (JNF) as a part of the cooperative research program with the USDA Forest Service. It was conducted in the GIS center of the Hebrew University of Jerusalem. Special thanks are due to Adi Ben-Nun for technical support with the GIS. We thank Curtis Flather and John Dymond for reviewing a previous version of the manuscript. Erez Tzfati and Ofer Zilberstein provided help in the photomap preparation.

References

Anon. 1994. *User guide for the Magellan GPS ProMARK X CP*. Magellan Systems Corporation, San Dimas, CA.

Anon. 1995. *ERDAS IMAGINE version 8.4 field guide*. ERDAS Inc., Atlanta, GA.

Anon. 1996. *Arc/Info 7.0.4 Users Guide*. Environmental Systems Research Institute (ESRI), Redlands, CA.

Aaviksoo, K. 1995. Simulating vegetation dynamics and land use in a mire landscape using a Markov model. *Landscape Urb. Plan.* 31: 129-142.

Akashi, Y. & Mueller-Dombois, D. 1995. A landscape perspective of the Hawaiian rain forest dieback. *J. Veg. Sci.* 6: 449-464.

Bakker, J.P., Willems, J.H. & Zobel, M. 1996. Long-term vegetation dynamics. Introduction. *J. Veg. Sci*. 7: 147-156.

Berger, R.P. & Baydack, R.K. 1992. Effects of aspen succession on sharp-tailed grouse, *Tympanuchus phasianellus*, in the Interlake Region of Manitoba. *Can. Field Natur.* 106: 185-191.

Biging, G.S., Congalton, R.G. & Murphy, E.C. 1991. A comparison of photo-interpretation and ground measurements of forest structure. *ACSM-ASPRS Annual Convention Technical Papers* 3: 6-15.

Bolstad, P.V. 1992. Geometric errors in natural resource GIS data: tilt and terrain effects in aerial photographs. *For. Sci.* 38: 367-380.

Callaway, R.M. & Davis, F.W. 1993. Vegetation dynamics, fire, and the physical environment in coastal central California. *Ecology* 74: 1567-1578.

Congalton, R.G. 1991. A review of assessing the accuracy of classifications of remotely sensed data. *Rem. Sens. Environ.* 37: 35-46.

Congalton, R.G. & Green, K. 1993. A practical look at the sources of confusion in error matrix generation. *Photogramm. Eng. Remote Sens.* 59: 641-644.

Debussche, M., Escarré, J., Lepart, J., Houssard, C. & Lavorel, S. 1996. Changes in Mediterranean plant succesion: old fields revisited. *J. Veg. Sci*. 7: 519-526.

Dymond, J.R. 1986. Digital photomaps from aerial photographs. *New Zeal. J. Technol.* 2: 143-148.

Dymond, J.R. 1988. Nonparametric modeling of radiance in hill country. *Remote Sens. Environ.* 25: 3-21.

Dymond, J.R. 1992. Nonparametric modeling of radiance in hill country for digital classification of aerial photographs. *Remote Sens. Environ.* 39: 95-102.

Dymond, J.R. & Trotter, C.M. 1997. Directional reflectance of vegetation measured by a calibrated digital camera. *Appl. Optics* 36: 18.

Frelich, L.E. & Reich, P.B. 1995. Spatial patterns and succession in a Minnesota southern-boreal forest. *Ecol. Monogr.* 65: 325-346.

Harrington, G.N. & Sanderson, K.D. 1994. Recent contraction of wet sclerophyll forest in the wet tropics of Queensland due to invasion by rainforest. *Pac. Conserv. Biol.* 1: 319-327.

Hester, A.J., Miller, D.R. & Towers, W. 1996. Landscape scale vegetation change in the Cairngorms. *Biol. Conserv.* 77: 41-51.

Johnson, W.C. 1994. Woodland expansion in the Platte river, Nebraska: patterns and causes. *Ecol. Monogr.* 64: 45-84.

Johnston, C.A. & Naiman, R.J. 1990. The use of a geographic information system to analyze long-term landscape alteration by beaver. *Landscape Ecol.* 4: 5-20.

Keane, R.E., Long, D.G., Basford, D. & Levesque, B.A. 1997. Simulating vegetation dynamics across multiple scales to assess alternative management strategies. *11th Annual Symposium on Geographic Information Systems*. Vancouver, Canada.

Ross, M.S., O'Brien, J.J. & Da-Silveira-Lobo-Sternberg, L. 1994. Sea-level rise and the reduction in pine forests in the Florida Keys. *Ecol. Appl.* 4: 144-156.

Scanlan, J.C. & Archer, S. 1991. Simulated dynamics of succession in a North American subtropical *Prosopis* savanna. *J. Veg. Sci.* 2: 625-634.

Short, D. & Short, D. 1987. Studying long term community dynamics using image processing. In: Tenhunen, J.D. (ed.) *Plant response to stress in Mediterranean climates*, pp. 165-171. Springer-Verlag, Berlin.

Sokal, R.R. & Rohlf, F.J. 1981. *Biometry*. Freeman and Co., New York, NY.

Stephens, P.R. 1985. Measuring changes in areal extent of bare sand-dunes using digital image analysis. *Conference proceedings of NZSSS/NZASC Soil Dynamics and Land Use Seminar*, pp. 368-379. Blenheim.

Strong, A.M. & Bancroft, G.T. 1994. Patterns of deforestation and fragmentation of mangrove and deciduous seasonal forests in the Upper Florida Keys. *Bull. Marine Sci.* 54: 795-804.

Teillet, P.M., Guindon, B. & Goodenough, D.G. 1982. On the slope-aspect correction of multispectral scanner data. *Can. J. Remote Sens.* 8: 84-106.

Tomaselli, R. 1977. The degradation of the Mediterranean maquis. *Ambio* 6: 356-362.

Woien, H. 1995. Deforestation, information and citations: a comment on environmental degradation in highland Ethiopia. *GeoJournal* 37: 501-511.

Received 7 August 1997;
Revision received 23 April 1998;
Accepted 23 April 1998.